Cancer Chemother Pharmacol (2009) 65:41–54
DOI 10.1007/s00280-009-1001-1

ORIGINAL ARTICLE

ABT-737, a BH3 mimetic, induces glutathione depletion and oxidative stress

Adrienne N. Howard · Kathleen A. Bridges · Raymond E. Meyn · Joya Chandra

Received: 22 December 2008 / Accepted: 5 April 2009 / Published online: 29 April 2009

Abstract
Purpose This study assessed the role of oxidative stress and loss of glutathione in ABT-737-induced apoptosis.
Methods Jurkat human acute lymphocytic leukemia cells and HeLa cells transfected with a tet-regulated Bcl-2 expression system were treated with ABT-737 or its less active stereoisomer. GSH concentrations, intracellular reactive oxygen species (ROS), caspase activation and apoptotic DNA fragmentation were measured.
Results ABT-737 induced oxidative stress through decreased GSH and increased intracellular hydrogen peroxide and superoxide levels. Apoptotic DNA fragmentation and caspase activation were the consequences of this oxidative stress. Combining ABT-737 with ROS-inducing agents such as adaphostin or etoposide enhanced cell death.
Conclusions These results demonstrate that inhibition of Bcl-2 causes a loss of GSH, an increase in ROS, caspase activation and subsequent apoptosis. Clinically, redox alterations as a consequence of Bcl-2 inhibition by ABT-737 should be considered in devising combination therapies with this novel agent or its derivatives.

Keywords ABT-737 · Bcl-2 · Apoptosis · ROS · Glutathione

A. N. Howard · J. Chandra (✉)
Department of Pediatrics Research,
The University of Texas M. D. Anderson Cancer Center,
Box 853, 1515 Holcombe Blvd, Houston, TX 77030, USA
e-mail: jchandra@mdanderson.org

K. A. Bridges · R. E. Meyn
Department of Experimental Radiation Oncology,
The University of Texas M. D. Anderson Cancer Center,
Houston, TX 77030, USA

Abbreviations

GSH	Glutathione
ALL	Acute lymphocytic leukemia
NAC	*N*-acetyl cysteine
HE	Dihydroethidium
H_2DCFDA	Dihydrodichlorofluorescein-diacetate
DCF	Dichlorofluorescein
OPA	*O*-Phthaldialdehyde
PI	Propidium iodide
ROS	Reactive oxygen species
CI	Combination index
CFTR	Cystic fibrosis transmembrane conductance regulator

Introduction

The anti-apoptotic protein, Bcl-2, has been found to be overexpressed in many tumors, thereby contributing to the survival of cancer cells [1]. Consequently, molecularly targeted therapies directed towards Bcl-2 have emerged as candidates for early clinical trials [20]. ABT-737 (Abbott Laboratories, Abbott Park, IL) is one such agent and is a small molecule inhibitor of several anti-apoptotic members of the Bcl-2 family, including Bcl-2, Bcl-w and Bcl-xL. ABT-737 functions as a BH3 mimetic—by binding to the BH3 domains of these anti-apoptotic proteins, preventing them from binding and inhibiting the pro-apoptotic Bcl-2 family members [24]. In vitro single agent activity by ABT-737 has been shown in small cell lung carcinoma, lymphoma, multiple myeloma and acute myeloid and lymphoid leukemia [12, 15, 24, 29], correlating with increased Bcl-2 expression in these malignancies. In tumor models where single agent activity was not observed, the hypothesis has been posed that ABT-737s inhibition of the anti-apoptotic

Bcl-2 family members could increase the sensitivity of cancer cells to apoptosis, at which point chemotherapeutic agents could be added and could act synergistically with ABT-737 [12]. In support of this concept, ABT-737 has been shown to enhance the cytotoxicity of vincristine, dexamethasone and L-asparaginase in acute lymphocytic leukemia cells [12].

Improved understanding of the mechanism by which Bcl-2 protects against apoptosis will aid in devising more effective strategies to target this oncogene. Bcl-2 and other anti-apoptotic family members are generally thought to prevent apoptosis by heterodimerizing with pro-apoptotic family members [26]. Bax and Bak are the examples of these pro-apoptotic family members and function by oligomerizing in mitochondrial membranes, leading to the release of cytochrome *c* and promoting caspase-9 and subsequent caspase-3 activation [27]. The localization of Bcl-2 to mitochondrial membranes is also suggestive of an effect on mitochondrial function, although no specific role in this regard has been delineated. However, numerous reports indicate that Bcl-2 expression is associated with an increase in the total cellular antioxidant capacity [17]. Because mitochondria are a major site of superoxide generation, mitochondrial localization of Bcl-2 could confer protection against oxidative stress [16]. Stronger support of this concept comes from studies in which Bcl-2 blocks apoptosis induced by hydrogen peroxide, menadione and γ-irradiation, all of which induce an oxidative stress [11]. Importantly, the overexpression of Bcl-2 in neuronal cells, lymphoma cells and ovarian cancer cells raises levels of intracellular GSH, the most abundant and ubiquitous cellular antioxidant [32].

In this study, we used ABT-737 as a tool with which to further test the relationship between Bcl-2 and redox status in a human ALL cell line and in HeLa cells containing a tetracycline (tet)-repressible system for Bcl-2 expression. We find that inhibition of Bcl-2 with ABT-737 lowered intracellular GSH levels, raised intracellular ROS and caused caspase-3-dependent apoptotic DNA fragmentation. Our data suggest a mechanism where inhibition of Bcl-2 by ABT-737 results in a decrease in intracellular GSH, thereby causing caspase activation and apoptosis. We also examined the potential activity of ABT-737 in combination with ROS-inducing chemotherapeutic agents, adaphostin [6, 34] and etoposide, a topoisomerase-II inhibitor, in an effort to apply this knowledge towards devising therapeutic strategies incorporating Bcl-2 inhibition.

Materials and methods

Reagents

ABT-737 and its stereoisomer were provided by Abbott Laboratories (Abbott Park, IL). The dyes dihydroethidium (HE), dihydrodichlorofluorescein-diacetate (H_2DCFDA) and 5-(and-6)-carboxyfluorescein diacetate (5(6)-CFDA) were purchased from Molecular Probes (Eugene, OR). Phenyl *N-t*-butylnitrone (PBN), *N*-acetyl-cysteine (NAC), etoposide and bovine glutathione peroxidase were purchased from Sigma (St Louis, MO). *O*-phthaldialdehyde (OPA) was purchased from Invitrogen (Carlsbad, CA). Adaphostin was kindly provided by Dr. Robert Schultz, Developmental Therapeutics Program, National Cancer Institute (Bethesda, MD). The antibody to Bcl-2 was purchased from Dako (Carpinteria, CA). The antibody to actin was purchased from Cell Signaling (Boston, MA). Anti-rabbit and anti-mouse HRP-conjugated secondary antibodies were purchased from Amersham Pharmacia Biotech (Piscataway, NJ). The pan-caspase inhibitor, zVAD-FMK and caspase substrate, Ac-DEVD-AMC, were purchased from Biomol International, LP (Plymouth Meeting, PA).

Cell culture

The Jurkat human ALL cell line was obtained from American Type Culture Collection (Rockville, MD) and maintained in RPMI 1640 medium supplemented with 10% (v/v) fetal bovine serum, 2 mM L-glutamine, 100 units/ml penicillin and 100 μg/ml streptomycin. HeLa S3 tet-off cells stably transformed with pTRE-Bcl-2 were generated as previously described [31]. Cells were grown in α-MEM without ribonucleosides or deoxyribonucleosides (GIBCO-BRL, Gaithersberg, MD) and supplemented with 10% (v/v) fetal bovine serum, 2 mM L-glutamine, 100 units/ml penicillin–streptomycin, 100 μg/ml hygromycin B (Calbiochem, San Diego, CA) and 200 μg/ml G418. To suppress Bcl-2 protein levels, HeLa cells containing the tet-regulated system were cultured in the presence of 1 μg/ml doxycycline (Sigma, St. Louis, MO) for 5 days and for this study are referred to as tet-on cells. Tet-off cells were cultured in the same conditions without doxycycline to allow Bcl-2 expression. Cell cultures were maintained at 37°C in a humidified atmosphere containing 5% CO_2 in air.

Measurement of glutathione levels

Intracellular GSH was measured based on the method by Hissin and Hilf [10]. HeLa cells were plated in 2–100 mm dishes at least 5 days prior to an experiment in order to regulate Bcl-2 expression and ultimately obtain 10×10^6 cells. HeLa and Jurkat cells were either left untreated or were treated with ABT-737, stereoisomer, or DMSO for 24 h prior to harvesting. The media from each treatment group was transferred to the appropriate tube, cells were washed twice with 5 ml phosphate-buffered saline (PBS) which was then also transferred to the corresponding tube and HeLa cells were trypsinized with 0.5 ml trypsin-EDTA. Cells

were harvested using 10 ml of the appropriate media and centrifuged at 1,100 rpm at 4°C for 10 min. The supernatant was aspirated and discarded and the cell pellet was rinsed twice with 0.1% saline solution. Cells were centrifuged again at 1,100 rpm at 4°C for 10 min and the supernatant discarded. Cells were then resuspended in lysis buffer [5% TCA: 1 mM EDTA: 0.1 N HCl (1:1:1, v/v/v)] at a density of 10×10^6 cells/ml lysis buffer, briefly vortexed and incubated on ice for 2 min. Samples were then centrifuged at 2,500*g* at 4°C for 20 min. The supernatant was transferred on to a clean Eppendorf tube and kept on ice.

Stock solutions of 1 mg/ml reduced glutathione (GSH) in EDTA, pH 8.0 and 1 mg/ml OPA in methanol stock solutions were freshly prepared in 15 ml tubes covered in foil and kept on ice. From the GSH stock solution, GSH standards were prepared at concentrations of 0, 0.1, 0.5, 1.0, 1.5, 2, 3, 5 and 10 μg/ml in order to generate a standard curve.

Standards and samples were prepared by adding 3.6 ml ice-cold EDTA, pH 8.0, 200 μl cold supernatant (or standard) and 200 μL ice-cold OPA to a glass tube. The tubes were vortexed briefly and incubated at room temperature in the dark for 15 min. The samples were read immediately on a Perkin Elmer LS 55 Luminescence Spectrometer using FL Winlab Molecular Spectroscopy Software version 4.00.02 at an excitation of 350 nm and an emission of 420 nm. Reduced GSH levels in the samples were calculated by standardization to the linear regression equation of the standard curve to determine concentration measured as μg/10×10^6 cells/ml, which was then converted to pg/cell. This method demonstrates specificity for reduced GSH versus oxidized GSSG because previous work has shown that adding *N*-ethylmaleimide to lysates prevents GSH oxidation. At pH 8.0, OPA-GSSG fluoresces at 0.1% the intensity of OPA-GSH [10, 19].

Western blot analysis

Total cellular extracts were prepared as previously described [31] and 30 μg of protein was applied to SDS-polyacrylamide (PAGE) electrophoresis. Proteins were separated electrophoretically on 12% SDS-PAGE gels and were then transferred onto polyvinylide difluoride membranes (Millipore, Billerica, MA). Membranes were blocked with constant agitation for 2 h at room temperature in 5% non-fat dry milk-TBS-T (50 mM Tris–PBS, pH 7.6, containing 0.1% Tween-20). Membranes were then probed with a 1:1,000 dilution of primary antibody in 5% milk-TBS-T at room temperature on a rocker for 1.5 h. Membranes were washed three times for 20 min each at room temperature in TBS-T and then incubated for 1.5 h at room temperature with horseradish peroxidase-conjugated secondary antibody at a 1:1,000 dilution. The membranes were then washed again in TBS-T three times for 20 min each at room temperature and the proteins detected by chemiluminescence with ECL plus Western Blotting Detection Reagents (Amersham Biosciences, Arlington Heights, IL) on a Typhoon 9400 scanner (Amersham Biosciences, Piscataway, NJ).

Measurement of ROS levels

Following exposure to diluent or ABT-737/stereoisomer, cells were stained with either 10 μM HE to measure intracellular superoxide, 10 μM H_2DCFDA in 1 ml media to measure intracellular hydrogen peroxide, or 10 μM 5(6)-CFDA as a redox-independent control. Cells were stained with either dye for 30 min at 37°C and fluorescence was measured using flow cytometry on a FACSCalibur (Becton Dickinson, Franklin Lakes, NJ). Data were analyzed with CellQuest software (Becton Dickinson, Palo Alto, CA). An additional assay for measuring superoxide was added in order to supplement the data obtained with HE, which can interact with DNA. Superoxide was measured using a chemiluminescence-based Superoxide Anion Detection Kit (Calbiochem, La Jolla, CA) per the manufacturer's instructions. One million Jurkat cells were treated with DMSO or with various doses of ABT-737 for 24 h. Cells were harvested, centrifuged and resuspended in fresh medium to a concentration of 500,000 cells per 100 μl. One hundred microliter of cell suspension was centrifuged and resuspended in 100 μl superoxide anion assay buffer. Luminol and enhancer solutions diluted in assay medium were added to final concentrations of 200 and 250 μM, respectively. Samples were transferred to polystyrene round-bottom tubes and light emission was recorded by a luminometer.

DNA fragmentation assay

To determine populations of sub-diploid cells, flow cytometric analysis was performed. Cells were pelleted by centrifugation, media were removed by aspiration and cells were then washed with PBS. After re-centrifugation, cells were resuspended in PBS containing 50 μg/ml propidium iodide (PI), 0.1% triton X-100 and 0.1% sodium citrate. Samples were analyzed via flow cytometry on the FL-3 channel of a Becton Dickinson FACSCalibur (Franklin Lakes, NJ). Data were analyzed using CellQuest software (Becton Dickinson, Palo Alto, CA).

Caspase-3 activity assay

Three million cells per sample were pelleted, resuspended in 150 μL PBS and lysed by freezing and thawing. Fifty microliters, representing one million cells, was loaded in triplicate on a 96-well plate. To each well, 150 μL of

50 μM DEVD-amc in DEVD buffer (10% sucrose, 0.001% IGEPAL, 0.1% 3-[(3-cholamidopropyl)dimethylamonio]-1 propyl sulfonate [CHAPS], 5 mM HEPES, pH 7.25) was added. The release of fluorescence (amc) was measured using a spectrofluorometer using an excitation of 355 nm and an emission of 460 nm. Fas-treated cells were used as positive controls for the assay.

Statistical analyses

All results represented mean ± standard deviation. Differences between treatments with: ABT-737 and its stereoisomer, the aforementioned compounds only and those compounds with NAC and the HeLa tet-on and HeLa tet-off were determined statistically using the student's paired *t* test. *P* values < 0.05 were considered significant. Combination indices (CI) were calculated using isobologram analysis based on the Chou and Talalay method with CalcuSyn software (Biosoft, Ferguson, MO) to determine synergy in experiments with ABT-737 and adaphostin [8]. CI values <1 indicated synergism and values <0.7 indicated strong synergism.

Results

ABT-737 diminishes levels of intracellular GSH

Previous data indicate that Bcl-2 overexpression raises intracellular GSH levels, thereby serving as a potential mechanism of protection against oxidative stress [23]. In order to test whether Bcl-2 inhibition with a small molecule would repress GSH levels, we exposed Jurkat cells, which are known to express Bcl-2, to increasing doses of ABT-737 and a less active stereoisomer of ABT-737 [24]. After a 24 h exposure to the indicated doses of ABT-737 or the stereoisomer, intracellular reduced GSH levels were quantified by fluorescent detection of OPA-GSH adducts (Fig. 1a). GSH levels steadily decreased with increasing concentrations of ABT-737, nearing 0 with the 10 μM treatment ($P < 0.05$ for all doses above 0.5 μM for ABT-737 versus control). Consistent with published reports of the stereoisomer having low levels of Bcl-2 inhibitory activity [24], GSH concentrations also decreased with the stereoisomer treatment, but not as substantially as with ABT-737 ($P < 0.01$ when comparing stereoisomer with ABT-737 at 5 and 10 μM). The initial studies of ABT-737 established doses ranging from 10 nM and 1 μM as effective in exerting Bcl-2 inhibitory properties such as promotion of cytochrome *c* release [24]. Importantly, the effects of ABT-737 on GSH levels are beginning to occur within this range, suggesting that the doses used are physiologically relevant.

To determine if GSH depletion by ABT-737 required Bcl-2 expression, we employed a human HeLa cervical cancer cell line stably transfected with a tetracycline repressible Bcl-2 expression construct [31]. In these HeLa cells, the presence of tetracycline (tet-on) downregulates ectopic Bcl-2 (Fig. 1b inset), whereas the removal of tetracycline (tet-off) permits ectopic Bcl-2 expression [33]. GSH levels were significantly lower in the tet-off cells (Fig. 1b and c, black bars), confirming previous studies linking Bcl-2 expression to GSH [23, 31]. With 1 μM ABT-737, GSH levels decreased approximately 50% in the Bcl-2-expressing tet-off cells (Fig. 1b) ($P < 0.001$). In the tet-on cells (Bcl-2 off), GSH levels did not change significantly with ABT-737 treatment. These data suggest that inhibition of ectopic Bcl-2 with ABT-737 induces depletion of GSH in a Bcl-2 expression specific manner.

Since a 1 μM exposure to ABT-737 decreased GSH, we tested exposure to a lower dose in Bcl-2 expressing tet-off HeLa cells to potentially identify different sensitivities to GSH depletion. Figure 1c shows GSH levels in cells treated with a 0.2 μM dose of ABT-737 for 24 h. GSH levels declined significantly ($P < 0.01$) in treated cells ectopically expressing Bcl-2 and less so in the tet-on (Bcl-2 off) cells. As a control, GSH levels were also measured in parental HeLa cells treated with doxycycline to rule out effects of doxycycline on GSH (Fig. 1d). The results show that addition of doxycycline had no significant effect on intracellular GSH.

Induction of oxidative stress by ABT-737

Figure 1 demonstrates that exposure to ABT-737 caused a reduction in intracellular GSH, which is the most abundant cellular defense against oxidative stress. Therefore, we investigated whether reduction of GSH via inhibition of Bcl-2 altered the redox environment by causing an increase in oxidative stress. Two distinct ROS were measured in cells exposed to ABT-737: hydrogen peroxide and superoxide. Jurkat cells were treated with various doses of either ABT-737 or its stereoisomer for 24 h. Cells were harvested and stained with H_2DCFDA and analyzed by flow cytometry to measure intracellular hydrogen peroxide (Fig. 2a). As ABT-737 concentration increased, so did values for DCF fluorescence, indicating an increase in intracellular hydrogen peroxide ($P < 0.05$ for all doses above 0.5 μM for ABT-737 versus control). Cell treatment with the stereoisomer caused a slight increase in mean fluorescence, but not to the degree induced by ABT-737 ($P < 0.05$ when ABT-737 treatment is compared with stereoisomer at all doses ≥1 μM). The inset histogram highlights DCF fluorescence in Jurkat cells treated with 5 μM ABT-737 (dotted line) or stereoisomer (lighter solid line).

To determine whether the increase in H_2O_2 was sustained after 24 h and whether longer treatment would result in ROS

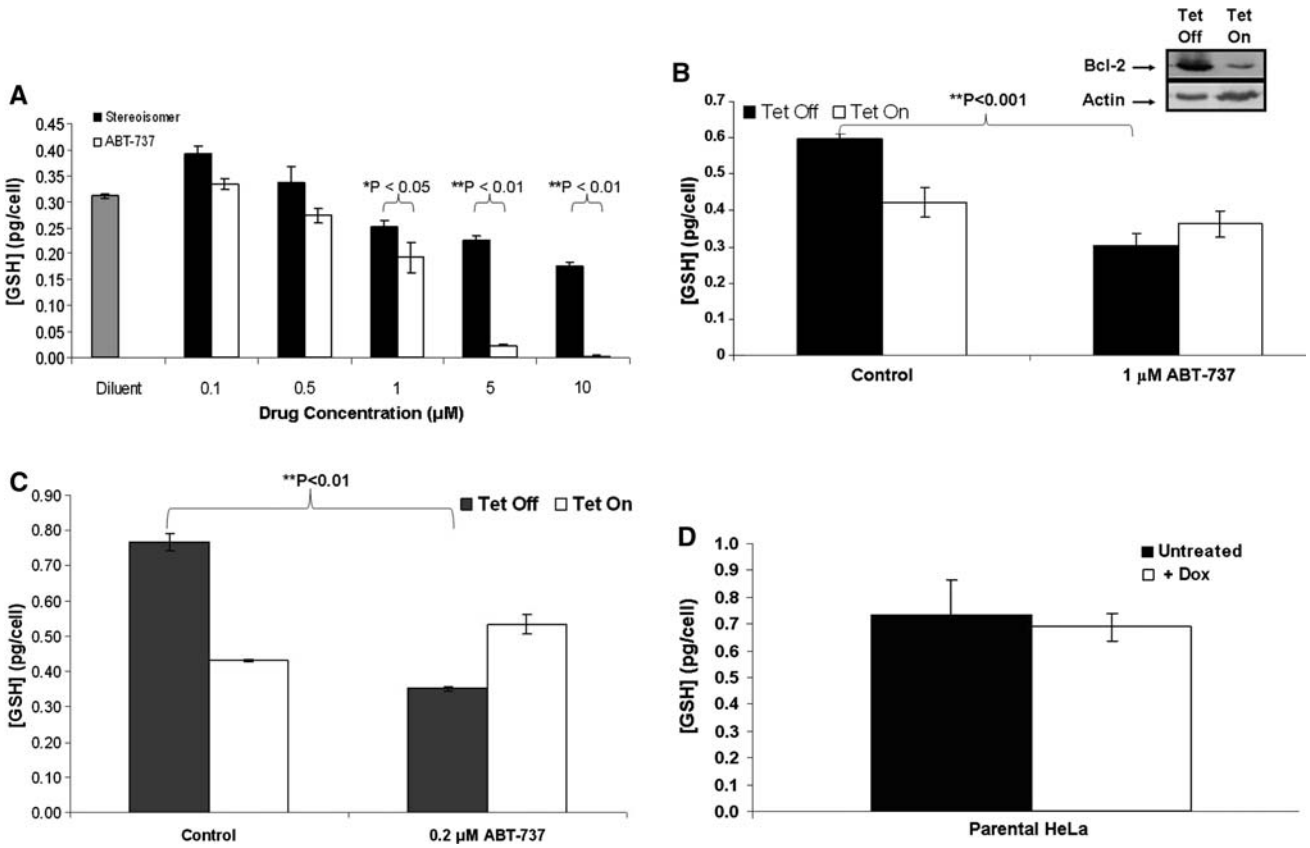

Fig. 1 Effects of ABT-737 on intracellular glutathione. **a** ABT-737 effects on glutathione in Jurkat cells. Jurkat cells were treated with diluent, 0.1, 0.5, 1, 5 or 10 μM of ABT-737 (*white bars*) or of stereoisomer (*black bars*) and GSH measurements were taken using a spectrofluorimeter as described in "Materials and methods". The *graph* depicts GSH concentrations in picograms/cell. $*P < 0.05$ for all doses above 1 μM for ABT-737 versus control. $**P < 0.01$ when comparing ABT-737 and stereoisomer. **b** and **c** GSH levels in HeLa cells expressing Bcl-2 decreased after treatment with ABT-737. HeLa cells with/without doxycycline (tet) removal (*inset* 1**b** shows Western blot of Bcl-2 protein expression) were treated with 1 μM (**b**) or 0.2 μM (**c**) ABT-737 for 24 h. Cells were lysed and GSH was measured using a spectrofluorimeter. *Bar graphs* depict averages from four independent experiments. $**P < 0.01$ when compared with control. **d** GSH levels are consistent in parental HeLa cells treated with or without doxycycline

induction with lower doses of ABT-737, DCF fluorescence was measured on cells treated with 0.1, 0.25, 0.5 and 1 μM ABT-737 following 36 and 48 h treatments (Fig. 2b). No increase in DCF fluorescence was observed with the lower doses (0.1 and 0.25 μM) at 36 (dotted line) or 48 h (solid line). A similar trend of increased fluorescence was seen at 36 h in cells treated with 0.5 and 1 μM ABT-737 as compared to cells treated with the same doses at 24 h (Figs. 2a, b) ($P < 0.05$ when compared with control). However at 48 h, there was very little increase in DCF fluorescence with 0.5 or 1 μM ABT-737 treatment, suggesting that increases in intracellular H_2O_2 do not persist from 36 to 48 h of treatment ($P < 0.05$ for 1 μM ABT-737 compared with control).

To rule out non-specific fluorescence of DCF in response to oxidation by reactive nitrogen species, a nitron-base spin trap, PBN, was employed. Jurkat cells were pretreated for 15 min with 100 μM PBN followed by the addition of various doses of ABT-737 for 24 h. Cells were stained with H_2DCFDA and analyzed by flow cytometry (Fig. 2c). Cells treated with the spin trap and ABT-737 had similar DCF fluorescence values to cells treated with ABT-737 alone, suggesting that the ROS entity being measured by H_2DCFDA is hydrogen peroxide as opposed to reactive nitrogen species.

To further confirm that ABT-737 was causing an increase in intracellular peroxides and not affecting dye influx, efflux or esterase cleavage, a redox-insensitive analog of H_2DCFDA, 5(6)-CFDA, was utilized. Cells were treated with 5 μM ABT-737 for 24 h. Also, cells treated with 1 mM H_2O_2 for 1 h were used as a positive control. Samples were harvested and stained with 10 μM of either H_2DCFDA or 5(6)-CFDA for 30 min. Flow cytometric analysis showed that DCF fluorescence increased in samples treated with the H_2O_2 positive control and with ABT-737 treatment (Fig. 2d) ($P < 0.05$ for H_2O_2 and $P = 0.01$ for ABT-737 when compared with control). CFDA fluorescence did not increase to the same extent as DCF, indicating that the redox sensitive properties of the compound were responsible for the increased fluorescence.

To measure intracellular superoxide, Jurkat cells were exposed to ABT-737 or its stereoisomer for 24 h, harvested and stained with dihydroethidium (Fig. 2e). After analysis with flow cytometry, cells treated with ABT-737 were found to have a higher percent increase in mean ethidium fluorescence than cells treated with the stereoisomer ($P < 0.05$ for all doses above 1 μM for ABT-737 versus stereoisomer). The dose-dependent increase in superoxide levels in ABT-737 treated cells began at the 0.5 μM dose and from there increased greatly with each increasing dose ($P < 0.05$ when comparing ABT-737 with control). As shown in Fig. 2a, the inset histogram highlights Jurkat cells treated with 5 μM ABT-737 or stereoisomer.

In order to determine whether increases in superoxide persist after 24 h and whether lower doses of ABT-737 can induce ROS with longer treatment, Jurkat cells were treated with 0.1, 0.25, 0.5 and 1 μM ABT-737 for 36 and 48 h followed by staining with dihydroethidium (Fig. 2f). Mean fluorescence values were determined by flow cytometric analysis. HE fluorescence of ABT-737 treated cells increased at both 36 and 48 h in a dose-dependent manner, with 1 μM ABT-737 treatment causing the greatest increase in mean fluorescence ($P \leq 0.01$ for doses greater than 0.25 μM at 48 h and 1 μM at 36 h when compared with controls, $P \leq 0.05$ for 0.1 and 0.5 μM compared with control at 36 h). These data indicated that an increase in superoxide levels occurs with lower doses (0.1 and 0.25 μM) at time points greater than 24 h (36 and 48 h) and increased superoxide levels persist following 0.5 and 1 μM treatment from 24 to 48 h.

A potential problem of using dihydroethidium as a measure of intracellular superoxide levels is its ability to react with DNA. Therefore, we employed a second measure of intracellular superoxide: Jurkat cells were treated with 1 or 5 μM ABT-737 for 24 h, harvested and incubated in a superoxide buffer containing a luminol reagent for 15 min. Luminescence values were recorded by a luminometer and percent increases in luminescence were graphed (Fig. 2g). Dose-dependent increases in luminescence were observed. Treatment with 1 μM ABT-737 caused an 80% increase in intracellular superoxide ($P < 0.01$) as compared to control and 5 μM treatment caused a 140% increase in superoxide levels ($P < 0.05$). Taken together, these data illustrate increases in both intracellular hydrogen peroxide and superoxide levels upon ABT-737 treatment.

Apoptotic DNA fragmentation and caspase activity correlate with induction of oxidative stress by ABT-737

Previous reports show that ABT-737 induces apoptosis in numerous cell lines and in in vivo mouse cancer models [12, 15, 24, 29]. To ensure that the cancer cell lines utilized in this study were sensitive to ABT-737-induced apoptosis, HeLa cells containing tet-regulated Bcl-2 were treated with 1 μM ABT-737 and its stereoisomer for 24 h. Cells were harvested and apoptotic sub-diploid populations were measured with propidium iodide staining and subsequent flow cytometric analysis (Fig. 3a). There was a 17% increase in the sub-diploid fraction in the tet-off cells, which did express ectopic Bcl-2 ($P < 0.05$), but not in the cells where ectopic expression of Bcl-2 was suppressed. It should also be noted that the tet-on cells displayed higher baseline levels of apoptosis presumably due to reduced levels of Bcl-2 expression as measured by Western blotting (Fig. 1b inset).

To determine whether the same doses of ABT-737 that lowered GSH and induced ROS were capable of inducing apoptosis in ALL cells, we treated Jurkat cells with increasing concentrations of ABT-737 or the stereoisomer for 24 h and measured apoptotic DNA fragmentation (Fig. 3b). When stained with PI and analyzed by flow cytometry, a noticeable increase in apoptotic cells occurred with 0.1 μM ABT-737 treatment, with cells undergoing apoptosis in a dose-dependent manner with increasing concentrations ($P < 0.05$ for all doses above 0.1 μM for ABT-737 versus

Fig. 2 ABT-737 causes an increase in ROS. **a** Intracellular hydrogen peroxide levels after treatment with ABT-737. Jurkat cells were treated with the indicated doses of ABT-737 (*solid line*) or stereoisomer (*dashed line*) for 24 h, harvested and stained with H_2DCFDA for 30 min before analysis by flow cytometry on the FL-1 channel. Mean DCF fluorescence is graphed to compare ROS levels. The representative histogram depicts diluent, 5 μM stereoisomer and 5 μM ABT-737. **b** Hydrogen peroxide levels increase at 36 h, but not 48 h. Jurkat cells were treated with the indicated doses of ABT-737 for 36 or 48 h followed by staining with H_2DCFDA as indicated above. Mean fluorescence values were measured by flow cytometry. **c** Spin trapping of reactive nitrogen species in combination with ABT-737 treatment results in similar increases in DCF fluorescence as treatment with ABT-737 alone. Cells were pretreated with 100 μM PBN for 15 min followed by treatment with various doses of ABT-737 for 24 h. Cells were harvested and stained with H_2DCFDA for 30 min followed by analysis of mean fluorescence on a flow cytometer. **d** Confirmation of specificity of H_2DCFDA in measuring reactive oxygen species. Jurkat cells were treated with 5 μM ABT-737 for 24 h or, as a positive control, 1 mM H_2O_2 for 1 h. Cells were stained with H_2DCFDA or its redox-insensitive analog, 5(6)-CFDA for 30 min followed by analysis of mean fluorescence on a flow cytometer. **e** Intracellular superoxides increase with ABT-737 treatment. Jurkat cells were treated with ABT-737 or stereoisomer for 24 h, harvested and stained with HE for 30 min before analysis by flow cytometry on the FL-3 channel. Percent increase in mean fluorescence was used to compare ROS levels. The *histogram* depicts the 5 μM treatment. **f** Superoxide levels increase with ABT-737 treatment at 36 and 48 h. Cells were treated with the indicated doses of ABT-737 for 36 and 48 h followed by HE staining. Mean fluorescence values were graphed to compare levels of superoxide. **g** Intracellular superoxide increases with ABT-737 treatment. Jurkat cells were treated with ABT-737 for 24 h, harvested, washed and resuspended in superoxide anion assay buffer. Luminol and enhancer reagents were added and luminescence values recorded after 15 min incubation. Percent increases in luminescence were used to compare superoxide levels. *$P < 0.05$ for all doses above 0.5 μM for ABT-737 versus control at 24 h. *$P < 0.05$, **$P < 0.01$ when comparing ABT-737 with stereoisomer at 24 h. *$P < 0.05$ and **$P < 0.01$ when comparing 36 and 48 h ABT-737 treatment with control

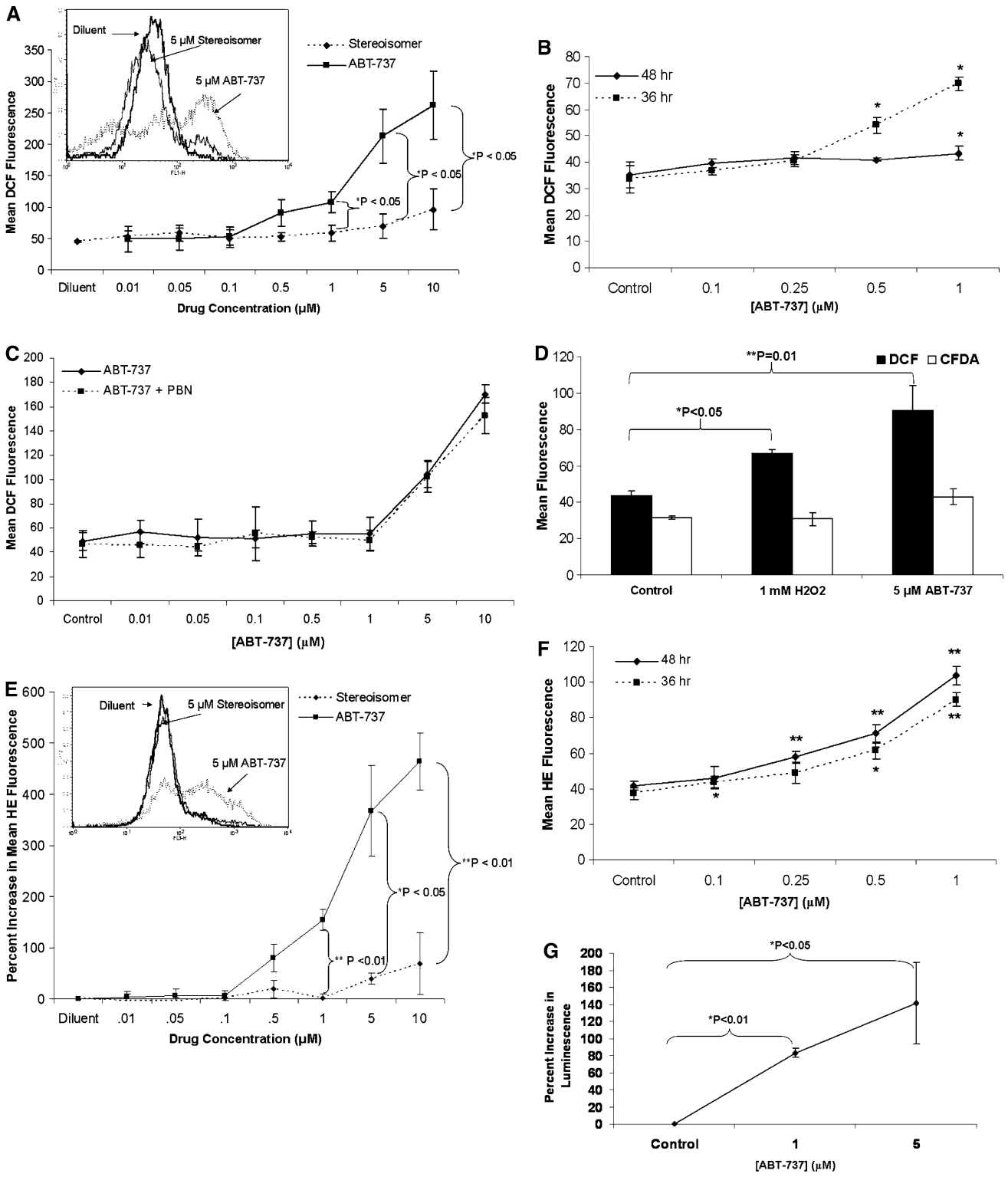

control). Dose-dependent sub-diploid populations were similar for samples treated for 36 and 48 h (data not shown) as compared to samples treated for 24 h (Fig. 3b), with the exception of 1 μM ABT-737 causing an approximate 10% increase at 36 and 48 h. The average percent of cells in sub-diploid populations from three experiments of 36-h treatments were 10.2, 15.5, 27.4 and 44.6% for 0.1, 0.25, 0.5 and 1 μM ABT-737, respectively. Average sub-diploid populations after 48 h of treatment were 12.1, 21.6, 31.0 and 47.4% for 0.1, 0.25, 0.5 and 1 μM ABT-737, respectively.

Caspase activity was then assessed to confirm apoptosis induction by ABT-737. To determine whether apoptosis

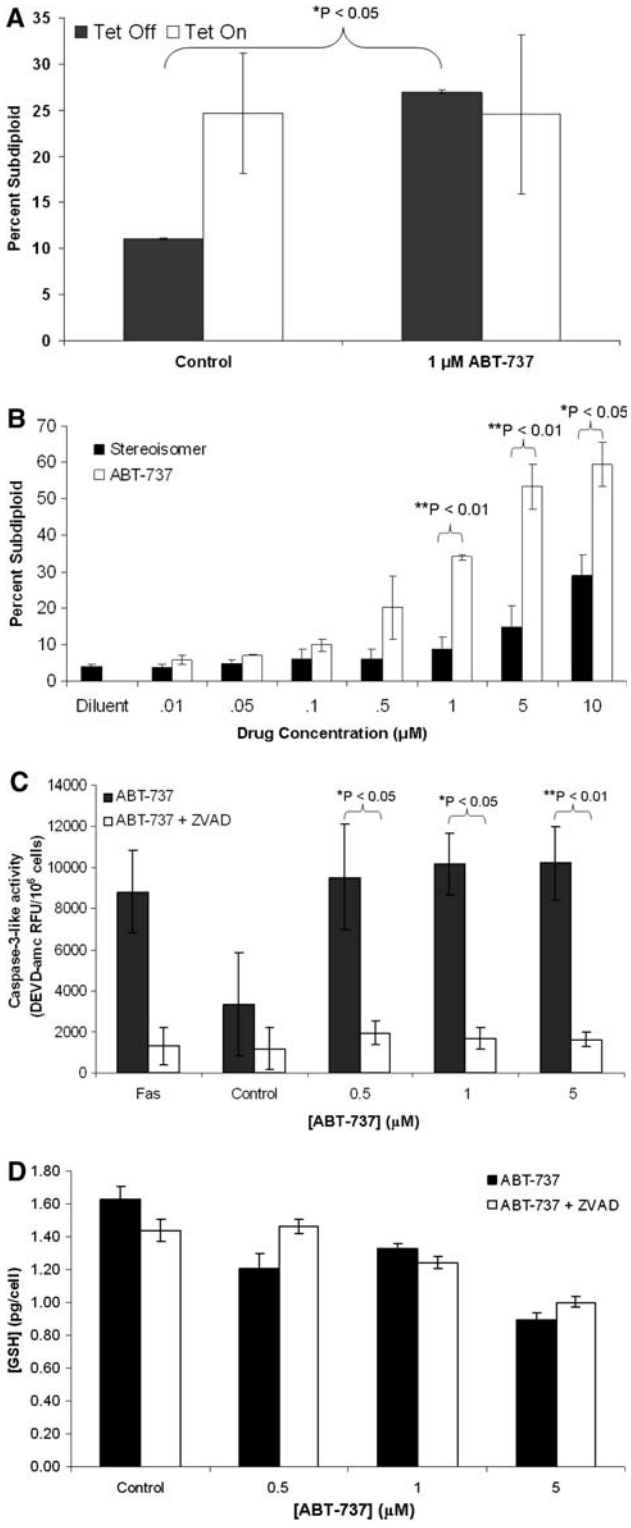

Fig. 3 ABT-737 induces apoptosis in a caspase-dependent manner. ▶ **a** DNA fragmentation by ABT-737 in HeLa cells. HeLa cells containing the tet-off system were treated with 1 μM ABT-737 or stereoisomer for 24 h and stained with PI. DNA fragmentation was assessed by flow cytometry on the FL-3 channel of a Becton Dickinson FACSCalibur. $*P < 0.05$ when compared with control. **b** ABT-737 produced an increase in the sub-diploid population of treated Jurkat cells. Cells were treated with increasing doses (0.01–10 μM) of ABT-737 (*white bars*) or its stereoisomer (*black bars*) for 24 h and then were stained with PI. Data shown are the results of three independent experiments. $*P < 0.05$ for all doses above 0.1 μM for ABT-737 versus control. $*P < 0.05$, $**P < 0.01$ when comparing ABT-737 with stereoisomer. **c** Caspase inhibition decreases ABT-737-induced caspase-3 activity. Jurkat cells were pretreated for 30 min with 10 μM zVAD followed by treatment with increasing doses of ABT-737 for 16 h. As a positive control, cells were treated with Fas antibody for 2 h prior to harvest. Caspase-3 activity was measured as described in "Materials and methods". $*P < 0.05$ for 0.5 and 1 μM ABT-737 and $**P < 0.01$ for 5 μM ABT-737 when compared with samples also treated with zVAD. **d** GSH reduction by ABT-737 is not a result of caspase activation. Jurkat cells were pretreated with zVAD for 30 min followed by the treatment with various doses of ABT-737 for 16 h. Cells were harvested and glutathione levels were measured as described in "Materials and methods"

induced by ABT-737 was caspase-dependent, Jurkat cells were pretreated with 10 μM zVAD, a pan-caspase inhibitor, for 30 min, followed by the addition of various doses of ABT-737 for 16 h. Two hour Fas antibody treatment of Jurkat cells was used as a positive control. The fluorogenic substrate, DEVD-AMC, was incubated with Jurkat cell lysates. Caspase-3-like activity, as indicated by AMC fluorescence, increased with ABT-737 treatment and decreased significantly in all samples pretreated with zVAD (Fig. 3c) ($P < 0.05$ for 0.5 and 1 μM ABT-737, $P < 0.01$ for 5 and 10 μM ABT-737). Apoptotic DNA fragmentation also decreased for all ABT-737-treated samples pretreated with zVAD (data not shown). These findings indicate that ABT-737-induced apoptosis is dependent upon caspase activation.

To place the observed decrease in intracellular GSH within the context of caspase activation and apoptosis in ABT-737-treated cells, we performed time course experiments examining DNA fragmentation, caspase-3 activity and GSH levels after ABT-737 treatment (data not shown). The results showed similar kinetics for caspase activation and GSH reduction, hence, a cause and effect relationship between these events was not clear from the time course experiments. Instead, to clarify whether decreases in GSH are dependent upon caspase activation, we measured GSH levels in Jurkat cells treated with ABT-737 or pretreated with the caspase inhibitor, zVAD, before the addition of ABT-737. Intracellular GSH was detected by measuring fluorescence of OPA-GSH adducts (Fig. 3d). The results showed no difference in samples treated with ABT-737 compared with samples pretreated with the caspase inhibitor, zVAD, suggesting that the ABT-737-induced drop in GSH occurs independently of caspase activation.

Decreases in GSH caused by ABT-737 enhance caspase-3 activity and DNA fragmentation

Because ABT-737 induces oxidative stress, loss of intracellular GSH and caspase activation, we examined whether the

antioxidant, NAC, would inhibit these effects of ABT-737. NAC is thought to exert its effects as an antioxidant either by acting as a GSH precursor—providing the cysteine necessary for GSH synthesis [2] or by acting as an antioxidant itself. We also used a chemical inhibitor of GSH, BSO, which acts by inhibiting γ-glutamylcysteine synthetase, the rate-limiting step in GSH synthesis. First, to confirm that both NAC and BSO modulate GSH, GSH levels were measured by OPA-GSH fluorescence after treatment of Jurkat cells with 24 mM NAC for 24 h or 1 mM BSO for 24 h (Fig. 4a, top). The results showed that BSO caused a complete depletion of intracellular GSH while NAC caused a ninefold increase in GSH, confirming that both chemicals functioned as expected. To provide assurance that the entity being measured by this assay is GSH and not other thiols, cell homogenates were treated with glutathione peroxidase (GPx) and OPA fluorescence was measured (Fig. 4a, bottom). The observed significant reduction in fluorescence in GPx treated samples indicated that GSH is the predominant thiol being assessed. Despite the use of uniform methodology (OPA assay) to measure intracellular GSH in Jurkat cells, we observed varying absolute values in untreated Jurkat cells in various experiments. In Jurkat cells, cell cycle variations in GSH content have been described by other investigators [28], providing a potential explanation for our results.

To determine whether antioxidant treatment would have an effect on ABT-737-induced caspase activation, Jurkat cells were treated with various doses of ABT-737 or were pretreated with 24 mM NAC for 1 h before the addition of ABT-737 for 16 h. Fas treatment was used as a positive control. Caspase-3-like activity was measured by AMC fluorescence and results show that addition of NAC reduces caspase activity significantly in samples treated with 0.5, 1 and 5 μM ABT-737 (Fig. 4b) ($P < 0.01$ for 0.5, 1 and 5 μM ABT-737 compared with ABT-737 plus NAC). Combined with the data shown in Fig. 4a showing that NAC raises GSH levels, this result suggests that GSH reduction occurs prior to caspase-3 activation with ABT-737 treatment.

Because ABT-737 causes an increased level of intracellular ROS, we tested the functional significance of this oxidative stress by using the antioxidant, NAC, to blunt ROS and examined effects on apoptotic DNA fragmentation. Jurkat cells were pretreated with 24 mM NAC for 30 min followed by the addition of 0.5 or 1 μM of ABT-737 (Fig. 4c). After 24 h, cells were harvested and stained with propidium iodide and analyzed by flow cytometry. NAC treatment caused a decrease in the ABT-737-induced sub-diploid population ($P < 0.05$ comparing ABT-737 alone to ABT-737 plus NAC).

Given our finding that ABT-737 causes a dose-dependent reduction of GSH levels, we tested the possibility that selective depletion of GSH with BSO (as shown in Fig. 4a) would enhance the apoptotic effects of ABT-737. Co-incubation of 1 mM BSO along with increasing doses of ABT-737 further enhanced apoptosis at specific doses (Fig. 4d) ($P < 0.05$ comparing 0.1 μM ABT-737 alone to ABT-737 plus BSO). Representative histograms are shown for control, 0.5 μM ABT-737, 1 mM BSO and combination of both.

ABT-737 synergizes with clinically relevant therapies that raise ROS levels

Since ABT-737 as a single agent increases ROS production, we sought to combine it with clinically relevant agents that also generate oxidative stress in an effort to potentially maximize its effects. Adaphostin is a ROS-inducing tyrphostin inhibitor with preclinical activity in leukemia, myeloma and brain tumor model systems [3, 4, 6, 25, 34]. Jurkat cells were treated with increasing doses of adaphostin (0.1, 0.5, 1 μM) together with increasing doses of ABT-737 (0.1, 0.5, 1 μM) for 24 h. Cells were harvested and stained with PI to measure DNA fragmentation. Figure 5a represents the percentage of cells in the sub-diploid population after exposure to three doses of ABT-737 plus 0.5 μM adaphostin ($P < 0.05$ when compared with ABT-737 alone). Greater than additive effects of the combined treatments were seen with several doses; 0.5 μM adaphostin plus either 0.5 μM or 1 μM ABT-737, as indicated by a combination index value of <1 (Table 1).

ABT-737 was further used in combination with etoposide, a topoisomerase-II inhibitor, shown to also generate ROS. ABT-737 or its stereoisomer at 0.2 μM doses were used in combination with 5 μM etoposide in HeLa cells ectopically expressing Bcl-2 (tet-off) for 24 h (Fig. 5b). Cells were then harvested and stained with PI. Etoposide alone caused a slight increase in apoptosis in tet-off cells. Etoposide plus stereoisomer caused no further increase in apoptosis, whereas etoposide treatment in combination with ABT-737 resulted in a substantial increase in apoptotic DNA fragmentation as compared to etoposide alone ($P < 0.01$).

Glutathione has the ability to reduce an etoposide phenoxyl radical that can be formed in cells with etoposide treatment, potentially resulting in decreased intracellular GSH [30]. Therefore, GSH levels were also measured in samples treated with ABT-737 in combination with etoposide. HeLa tet-off cells were treated with ABT-737, etoposide, or in combination as above. Cells were harvested and intracellular GSH was measured by OPA-GSH fluorescence (Fig. 5c). As also shown in Fig. 1c, GSH levels decreased with 0.2 μM ABT-737 ($P < 0.01$). GSH levels did not change with etoposide treatment. In samples treated with both ABT-737 and etoposide in combination, GSH levels decreased to the same degree as with ABT-737 alone ($P < 0.01$). These data suggest that the mechanism of synergy and ROS induction is not through the ability of both drugs to decrease GSH.

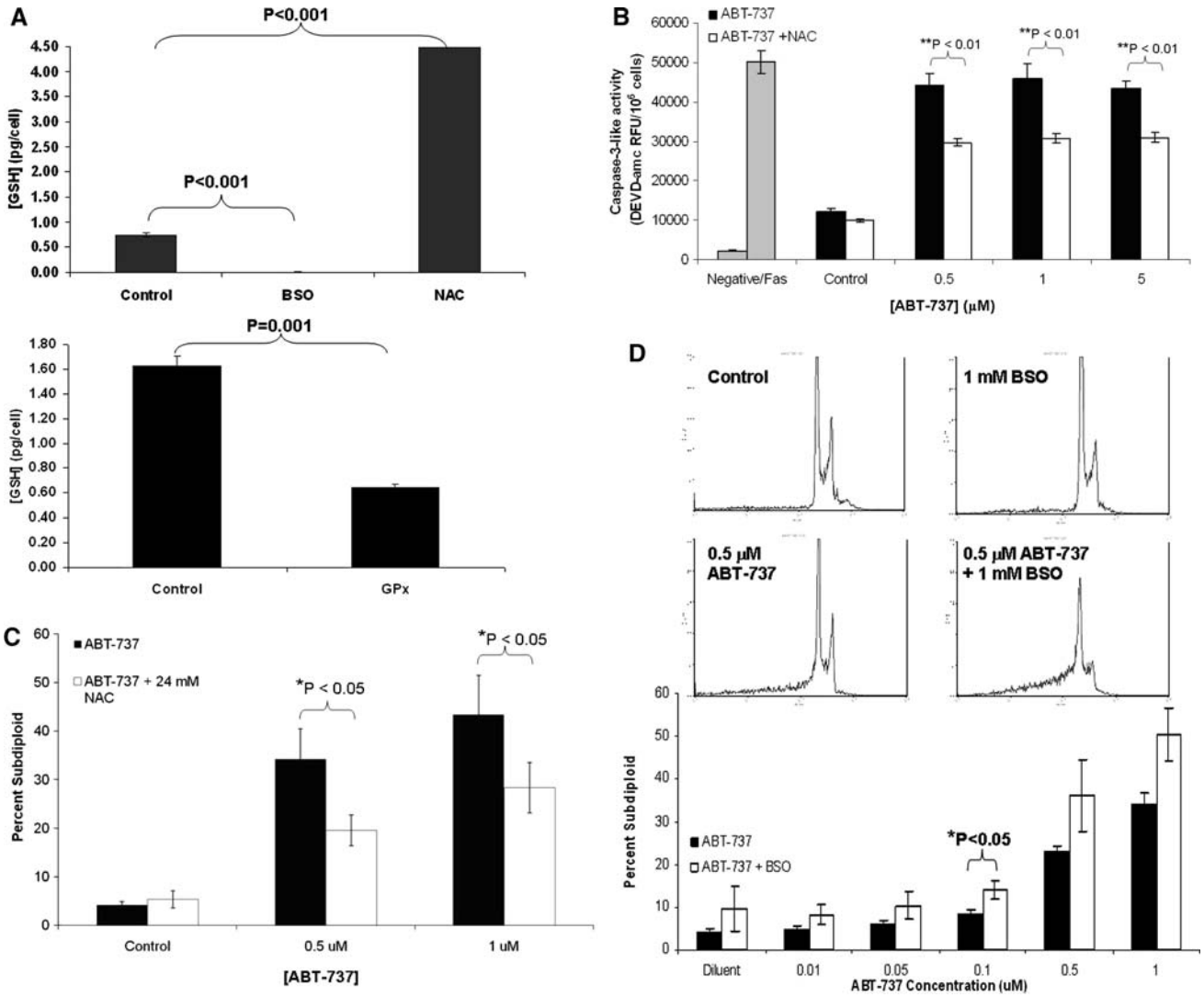

Fig. 4 Addition of NAC inhibits ABT-737 induced caspase activity and DNA fragmentation while BSO pretreatment augments DNA fragmentation. **a** NAC augments GSH levels while BSO and glutathione peroxidase decrease GSH levels in Jurkat cells. Cells were treated with 24 mM NAC or 1 mM BSO for 24 h followed by measurement of GSH concentration as described in "Materials and methods" (*top*). Cell homogenates were treated with 5 U glutathione peroxidase and 2 mM H_2O_2 for 5 min prior to addition of OPA in order to eliminate reduced GSH (*bottom*). *$P < 0.001$ when compared with control. **b** Addition of NAC inhibits caspase activation in ABT-737-treated cells. Jurkat cells were pretreated with 24 mM NAC for 30 min followed by 16-h treatment with various doses of ABT-737. Two hour Fas treatment served as a positive control. Cells were harvested and caspase-3 activity was measured as described in "Materials and methods". *$P < 0.01$ when comparing ABT-737 alone with ABT-737 plus NAC. **c** Antioxidant treatment inhibits ABT-737-induced DNA fragmentation. Jurkat cells were pretreated with 24 mM NAC for 30 min followed by treatment with ABT-737. Cells were harvested after 24 h and stained with PI and quantitated via flow cytometry on the FL-3 channel. *$P < 0.05$ when comparing ABT-737 alone with ABT-737 plus NAC. **D.** Depletion of glutathione with BSO augments ABT-737-induced apoptosis. Jurkat cells were pretreated with 1 mM BSO for 10 min followed by different doses of ABT-737 for 24 h. Cells were harvested and stained with PI. Sub-diploid populations were analyzed by flow cytometry. Histograms represent populations of cells treated with 0.5 μM ABT-737, 1 mM BSO, or with both together. *$P < 0.05$ when comparing the drug alone with drug plus BSO

Discussion

Bcl-2 and related anti-apoptotic family members are known to limit the efficacy of chemo- and radiotherapies in virtually any cell type [9]. The development of ABT-737 to specifically target Bcl-2 serves as validation of the well-documented role of this protein in protecting cancer cells against apoptosis. Numerous studies have linked Bcl-2 to increased or redistributed GSH [22, 23, 31]. We find that ABT-737 treatment in Jurkat ALL cells induces oxidative stress and apoptosis, which coincides with a reduction in GSH levels. The concept of combining Bcl-2 targeted therapies with

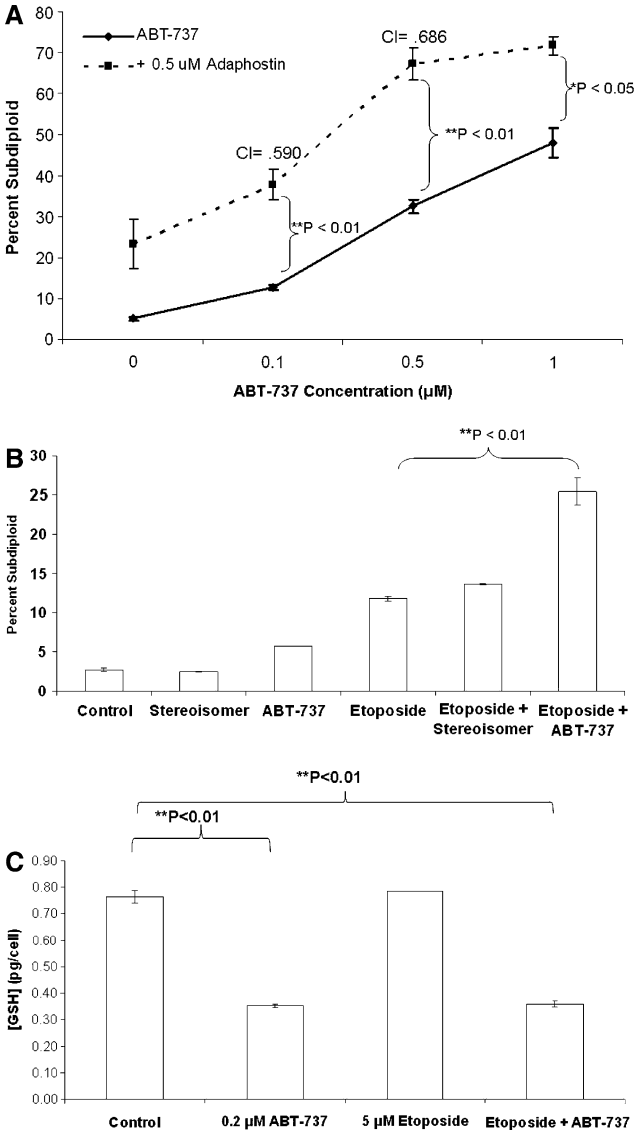

Fig. 5 ABT-737 potentiates cell death when combined with agents that raise ROS levels. **a** ABT-737 in combination with adaphostin potentiates apoptosis in Jurkat cells. Cells were treated with 0.1, 0.5 or 1 μM of both adaphostin and ABT-737 for 24 h. Cells were harvested, stained with PI and analyzed on the FL-3 channel of a flow cytometer. The *graph* depicts the three doses of ABT-737 and the 0.5 μM dose of adaphostin. The results of the other adaphostin doses are shown in Table 1. Combination indices for these doses are indicated on the *graph*. $*P < 0.05$ and $**P < 0.01$ when comparing combination treatment with ABT-737 treatment alone. **b** Etoposide enhanced apoptotic effects of ABT-737 in HeLa cells. HeLa cells containing the tet-off system were treated with 0.2 μM ABT-737 and 5 μM etoposide. Cells were harvested after 24 h, stained with PI and analyzed on the FL-3 channel of a flow cytometer. $**P < 0.01$ when compared with etoposide alone. **c** GSH levels decrease in samples treated with the ABT-737 and etoposide combination to the same degree as ABT-737 treatment alone. HeLa tet-off/on cells were treated with 0.2 μM ABT-737 and 5 μM etoposide for 24 h. GSH content was determined by measurement of OPA-GSH adducts using a spectrofluorimeter as described in "Materials and methods. $**P < 0.01$ when comparing ABT-737 alone or combination treatment with etoposide with control

Table 1 Combination indices for ABT-737 and adaphostin

Adaphostin (μM)	ABT-737 or stereoisomer (μM)	CI ABT = 737 + adaphostin	CI stereoisomer + adaphostin
0.1	0.1	1.058	0.826
0.1	0.5	0.893	0.928
0.1	1	1.007	1.182
0.5	0.1	0.911	1.096
0.5	0.5	0.590	0.870
0.5	1	0.686	0.909
1	0.1	0.753	0.918
1	0.5	0.814	0.860
1	1	0.952	0.851

Indicated doses of adaphostin and either ABT-737 or the less active stereoisomer were combined in Jurkat cells

Drugs were dosed simultaneously for 24 h and apoptotic DNA fragmentation was assessed by PI staining

Effective fractions were determined by subtracting the average percentage of the control sub-diploid population from the average percentage of the treated sub-diploid population for each dose and then divided by 100

These values were entered into the CalcuSyn program along with the various doses of ABT-737/stereoisomer and adaphostin and their combinations

Combination indices were determined by CalcuSyn based on the Chou and Talalay method and are reported in the table next to their corresponding doses [8]

Synergy is indicated with values less than 1. Stronger synergy is seen with 0.5 μM adaphostin and either 0.5 or 1 μM ABT-737, which are highlighted in bold

GSH depleting agents has been tested using other compounds. A recent study has shown that antisense targeting of Bcl-2 using G3139 and depletion of GSH with verapamil can sensitize melanoma to combination therapies in vivo [21]. However, since verapamil is a potent inhibitor of P-glycoprotein, which potentiates the efflux of certain drugs, it is difficult to attribute the synergy as selectively due to GSH depletion in that study.

The precise relationship between Bcl-2 and GSH is not well understood. Since ABT-737 is a selective small molecule inhibitor of Bcl-2 binding to pro-apoptotic family members, it can be used to increase knowledge regarding the regulation of redox by Bcl-2. Increased levels of the antioxidant GSH have been found to correlate with overexpression of Bcl-2 and Bcl-2 is thought to inhibit the cellular efflux of GSH [22]. Since GSH efflux from the cell prior to apoptosis commitment has been observed in some cell lines and may contribute to the increase in ROS observed in some apoptotic models, Bcl-2s protective effects may be through prevention of this efflux. Recent works highlight a role for the cystic fibrosis transmembrane conductance regulator (CFTR) in GSH extrusion and identifies Bcl-2 as a direct or indirect

inhibitor of CFTR-mediated GSH efflux [5]. Separate studies have addressed the ability of Bcl-2 inhibitors (HA14-1 and compound 6) to deplete mitochondrial GSH [35], which constitutes approximately 10% of total cellular GSH, in rat cerebellar granule neurons. Actual binding of GSH to Bcl-2 at the BH3 domain is cited as the mechanism for this observation [35], yet it is unclear whether mitochondrial GSH and non-mitochondrial GSH share this binding ability. Since our assessments of GSH levels measured total cellular GSH (Fig. 1a–c) and were inclusive of mitochondria, the ability of ABT-737 to deplete this larger GSH pool appears more consequential for cell fate.

Our results show that ABT-737 raises ROS levels in Jurkat cells with substantial increases in hydrogen peroxides and superoxides (Fig. 2). GSH functions as a reducing agent during the conversion of hydrogen peroxide to water and oxygen [11]. After ABT-737 treatment, depleted GSH levels in the Jurkat cells (Fig. 1a) could be contributing to the accumulation of these reactive oxygen species (ROS). Accordingly, the pretreatment with NAC, which acts as an antioxidant alone or by providing cysteine for GSH synthesis [2], diminished ABT-737-induced caspase-3 activity and apoptosis compared with ABT-737 treatment alone (Figs. 4b, c) and GSH depletion with BSO also enhanced ABT-737-induced apoptosis (Fig. 4d), providing further evidence that GSH levels are important in regulating the ABT-737 induced apoptotic pathway. With regard to ROS induction, both superoxide and hydrogen peroxide are generated with $\geq$0.5 μM ABT-737 at 24 h. Although superoxide generation persists up to 48 h (Fig. 2f), increases hydrogen peroxide were only observed up to 36 h (Fig. 2b). Potential explanations for these observations include persistent superoxide production by the mitochondria as a result of Bcl-2 inhibition or an increase in $H_2O_2^-$ scavenging enzyme activity after 24 h.

In vivo studies have found that ABT-737 alone can induce regression of solid tumors such as lymphoma and small-cell lung carcinoma [24]. Other in vitro work shows that ABT-737 can induce apoptosis in multiple myeloma [13] and acute leukemia systems [15]. Our results showed that ABT-737 induced apoptosis in Jurkat human ALL cells at the same doses used to generate an oxidative stress (Fig. 3b). ABT-737s stereoisomer also caused apoptosis, but to a lesser extent, due to a lower Bcl-2 inhibitory activity of the stereoisomer. Interestingly, ABT-737 also induced apoptosis in HeLa cells where ectopic expression of Bcl-2 was suppressed (Fig. 3a). Apoptosis in HeLa cells with downregulated Bcl-2 could be the result of ABT-737s additional targeting of other anti-apoptotic molecules, including Bcl-w and Bcl-xL or inhibition of the basal level of Bcl-2 in HeLa cells (Fig. 1b inset). We also found that increases in apoptosis did not occur in Bax/Bak double knockout murine embryonic fibroblasts treated with 1 μM ABT-737 (data not shown), suggesting that upon inhibition of Bcl-2 with ABT-737, Bax and Bak are free to oligomerize and activate the apoptotic pathway.

Studies have shown that ABT-737 induces caspase cleavage, which leads to the execution of apoptosis, in multiple cell lines [7, 13, 29]. Our data shows that ABT-737 induces caspase-3 activation in Jurkat cells and this activation is inhibited by the pan-caspase inhibitor, zVAD-fmk (Fig. 3c), and by the GSH precursor, NAC (Fig. 4b). Inhibition of caspases with zVAD had no effect on reduced GSH levels caused by ABT-737 (Fig. 3d), suggesting this loss of GSH occurs prior to caspase activation. These data further show that ABT-737-induced apoptosis is caspase-dependent and that reduction of intracellular GSH is important for ABT-737-induced caspase activation and subsequent apoptosis. However, time course studies revealed caspase-3 activity and GSH depletion occurring within similar time frames, which makes ordering of events a difficult task. Nonetheless, the inability of a pan-caspase inhibitor, zVAD-fmk, to impact GSH loss by ABT-737 indicates that GSH depletion is an earlier event than caspase activation. A proposed mechanism of GSH depletion and activation of apoptosis is shown in Fig. 6. When ABT-737 binds to the BH3 domain of anti-apoptotic Bcl-2 family members, Bcl-2

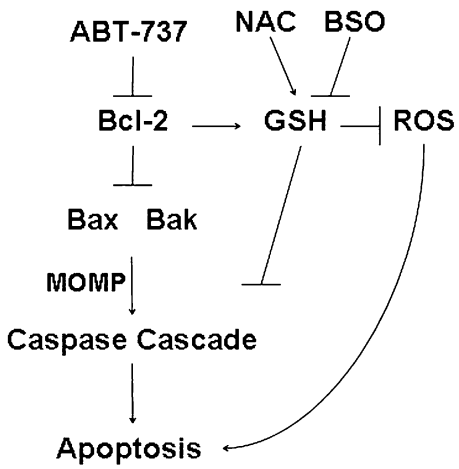

Fig. 6 Proposed mechanism of ABT-737-induced apoptosis. The results from this study suggest that inhibition of Bcl-2 with the small molecule BH3 mimetic, ABT-737, induces apoptosis through a mechanism involving the antioxidant, GSH and generation of ROS. Following inhibition of Bcl-2 with ABT-737, GSH levels decrease by two possibilities: direct modulation of GSH levels by Bcl-2 or facilitation of extrusion when Bcl-2 is inhibited. Pro-apoptotic family members that are usually inhibited by binding to Bcl-2 are able to oligomerize and become activated. This leads to mitochondrial outer membrane permeabilization, resulting in cytochrome *c* release and generation of ROS. Decreased GSH levels contribute to increased ROS since cellular antioxidant capacity is lost. Once cytochrome *c* is released, traditional apoptotic events occur, such as activation of the caspase cascade. Therefore, we propose that ABT-737 induces caspase activation and apoptosis, at least in part, through generation of ROS and loss of intracellular GSH

is unable to suppress oligomerization of Bax and Bak and subsequent mitochondrial membrane permeability. Inhibition of Bcl-2 also results in a loss of intracellular GSH, either through direct interaction with GSH or by facilitating its extrusion from the cell, resulting in a decreased antioxidant capacity and an increase in ROS. ROS are also likely generated directly from mitochondria. Through an unknown mechanism, drops in GSH levels appear to be necessary for caspase activation and execution of apoptosis, providing evidence for the importance of ROS generation and GSH depletion in ABT-737-induced cell death.

ABT-737 has been found to synergize with several different drugs. Apoptosis induction by INNO-406, a second-generation Bcr-Abl kinase inhibitor, was enhanced with ABT-737 treatment in Bcr-Abl + leukemia, as reported in one study [18]. Other investigators have shown that ABT-737 works well as a single agent or in combination with dexamethasone or melphalan [29]. In another study with acute myeloid leukemia cells, synergistic effects were seen with ABT-737 in combination with Nutlin-3a [14]. Based on our observations of ROS production and the drop in GSH following ABT-737 treatment, we chose to combine the ROS-inducing agents, adaphostin or etoposide, with ABT-737. The rationale for this strategy was that theoretically, by inducing more ROS with the combination treatment, cells would be overwhelmed and apoptosis would be potentiated, which is in fact what we saw (Fig. 5; Table 1). Our results, along with additive/synergistic effects seen by others, indicate that ABT-737 could be an effective agent for leukemia either alone or in combination in vivo.

In summary, we conclude that ABT-737, alone or in combination with ROS-generating chemotherapies, shows preclinical efficacy in ALL cells and in Bcl-2-over-expressing cervical cancer cells. Consistent with Bcl-2 effects on GSH, our data indicates that part of ABT-737s mechanism of action is to lower GSH levels through Bcl-2 inhibition, which then permits generation of ROS, followed by caspase activation and apoptosis. Further studies of the effects of ABT-737 and its clinically related analogs in combination with agents that cause oxidative stress or GSH depletion will be helpful in designing more effective treatments for leukemia and other cancers.

Acknowledgments This work was supported in part by RO1 CA69003 to R.M. and RO1 CA115811 to J.C.

References

1. Adams JM, Cory S (2007) The Bcl-2 apoptotic switch in cancer development and therapy. Oncogene 26:1324–1337
2. Atkuri KR, Mantovani JJ, Herzenberg LA, Herzenberg LA (2007) *N*-Acetylcysteine–a safe antidote for cysteine/glutathione deficiency. Curr Opin Pharmacol 7:355–359
3. Avramis IA, Christodoulopoulos G, Suzuki A, Laug WE, Gonzalez-Gomez I, McNamara G, Sausville EA, Avramis VI (2002) In vitro and in vivo evaluations of the tyrosine kinase inhibitor NSC 680410 against human leukemia and glioblastoma cell lines. Cancer Chemother Pharmacol 50:479–489
4. Avramis IA, Laug WE, Sausville EA, Avramis VI (2003) Determination of drug synergism between the tyrosine kinase inhibitors NSC 680410 (adaphostin) and/or STI571 (imatinib mesylate, Gleevec) with cytotoxic drugs against human leukemia cell lines. Cancer Chemother Pharmacol 52:307–318
5. Benlloch M, Ortega A, Ferrer P, Segarra R, Obrador E, Asensi M, Carretero J, Estrela JM (2005) Acceleration of glutathione efflux and inhibition of gamma-glutamyltranspeptidase sensitize metastatic B16 melanoma cells to endothelium-induced cytotoxicity. J Biol Chem 280:6950–6959
6. Chandra J, Hackbarth J, Le S, Loegering D, Bone N, Bruzek LM, Narayanan VL, Adjei AA, Kay NE, Tefferi A, Karp JE, Sausville EA, Kaufmann SH (2003) Involvement of reactive oxygen species in adaphostin-induced cytotoxicity in human leukemia cells. Blood 102:4512–4519
7. Chauhan D, Velankar M, Brahmandam M, Hideshima T, Podar K, Richardson P, Schlossman R, Ghobrial I, Raje N, Munshi N, Anderson KC (2007) A novel Bcl-2/Bcl-X(L)/Bcl-w inhibitor ABT-737 as therapy in multiple myeloma. Oncogene 26:2374–2380
8. Chou TC, Talalay P (1984) Quantitative analysis of dose–effect relationships: the combined effects of multiple drugs or enzyme inhibitors. Adv Enzyme Regul 22:27–55
9. Cotter FE (2004) Unraveling biologic therapy for Bcl-2-expressing malignancies. Semin Oncol 31:18–21 discussion 33
10. Hissin PJ, Hilf R (1976) A fluorometric method for determination of oxidized and reduced glutathione in tissues. Anal Biochem 74:214–226
11. Hockenbery DM, Oltvai ZN, Yin XM, Milliman CL, Korsmeyer SJ (1993) Bcl-2 functions in an antioxidant pathway to prevent apoptosis. Cell 75:241–251
12. Kang MH, Kang YH, Szymanska B, Wilczynska-Kalak U, Sheard MA, Harned TM, Lock RB, Reynolds CP (2007) Activity of vincristine, L-ASP, and dexamethasone against acute lymphoblastic leukemia is enhanced by the BH3-mimetic ABT-737 in vitro and in vivo. Blood 110:2057–2066
13. Kline MP, Rajkumar SV, Timm MM, Kimlinger TK, Haug JL, Lust JA, Greipp PR, Kumar S (2007) ABT-737, an inhibitor of Bcl-2 family proteins, is a potent inducer of apoptosis in multiple myeloma cells. Leukemia 21:1549–1560
14. Kojima K, Konopleva M, Samudio IJ, Schober WD, Bornmann WG, Andreeff M (2006) Concomitant inhibition of MDM2 and Bcl-2 protein function synergistically induce mitochondrial apoptosis in AML. Cell Cycle 5:2778–2786
15. Konopleva M, Contractor R, Tsao T, Samudio I, Ruvolo PP, Kitada S, Deng X, Zhai D, Shi YX, Sneed T, Verhaegen M, Soengas M, Ruvolo VR, McQueen T, Schober WD, Watt JC, Jiffar T, Ling X, Marini FC, Harris D, Dietrich M, Estrov Z, McCubrey J, May WS, Reed JC, Andreeff M (2006) Mechanisms of apoptosis sensitivity and resistance to the BH3 mimetic ABT-737 in acute myeloid leukemia. Cancer Cell 10:375–388
16. Korsmeyer SJ, Yin XM, Oltvai ZN, Veis-Novack DJ, Linette GP (1995) Reactive oxygen species and the regulation of cell death by the Bcl-2 gene family. Biochim Biophys Acta 1271:63–66
17. Kowaltowski AJ, Fiskum G (2005) Redox mechanisms of cytoprotection by Bcl-2. Antioxid Redox Signal 7:508–514
18. Kuroda J, Kimura S, Strasser A, Andreeff M, O'Reilly LA, Ashihara E, Kamitsuji Y, Yokota A, Kawata E, Takeuchi M, Tanaka R, Tabe Y, Taniwaki M, Maekawa T (2007) Apoptosis-based dual molecular targeting by INNO-406, a second-generation Bcr-Abl inhibitor, and ABT-737, an inhibitor of antiapoptotic

Bcl-2 proteins, against Bcr-Abl-positive leukemia. Cell Death Differ 14:1667–1677
19. Lash LH (2006) Mitochondrial glutathione transport: physiological, pathological and toxicological implications. Chem Biol Interact 163:54–67
20. Letai A (2005) BCL-2: found bound and drugged! Trends Mol Med 11:442–444
21. Mena S, Benlloch M, Ortega A, Carretero J, Obrador E, Asensi M, Petschen I, Brown BD, Estrela JM (2007) Bcl-2 and glutathione depletion sensitizes B16 melanoma to combination therapy and eliminates metastatic disease. Clin Cancer Res 13:2658–2666
22. Meredith MJ, Cusick CL, Soltaninassab S, Sekhar KS, Lu S, Freeman ML (1998) Expression of Bcl-2 increases intracellular glutathione by inhibiting methionine-dependent GSH efflux. Biochem Biophys Res Commun 248:458–463
23. Mirkovic N, Voehringer DW, Story MD, McConkey DJ, McDonnell TJ, Meyn RE (1997) Resistance to radiation-induced apoptosis in Bcl-2-expressing cells is reversed by depleting cellular thiols. Oncogene 15:1461–1470
24. Oltersdorf T, Elmore SW, Shoemaker AR, Armstrong RC, Augeri DJ, Belli BA, Bruncko M, Deckwerth TL, Dinges J, Hajduk PJ, Joseph MK, Kitada S, Korsmeyer SJ, Kunzer AR, Letai A, Li C, Mitten MJ, Nettesheim DG, Ng S, Nimmer PM, O'Connor JM, Oleksijew A, Petros AM, Reed JC, Shen W, Tahir SK, Thompson CB, Tomaselli KJ, Wang B, Wendt MD, Zhang H, Fesik SW, Rosenberg SH (2005) An inhibitor of Bcl-2 family proteins induces regression of solid tumours. Nature 435:677–681
25. Podar K, Raab MS, Tonon G, Sattler M, Barila D, Zhang J, Tai YT, Yasui H, Raje N, DePinho RA, Hideshima T, Chauhan D, Anderson KC (2007) Up-regulation of c-Jun inhibits proliferation and induces apoptosis via caspase-triggered c-Abl cleavage in human multiple myeloma. Cancer Res 67:1680–1688
26. Reed JC (2006) Proapoptotic multidomain Bcl-2/Bax-family proteins: mechanisms, physiological roles, and therapeutic opportunities. Cell Death Differ 13:1378–1386
27. Scorrano L, Korsmeyer SJ (2003) Mechanisms of cytochrome *c* release by proapoptotic BCL-2 family members. Biochem Biophys Res Commun 304:437–444
28. Soderdahl T, Enoksson M, Lundberg M, Holmgren A, Ottersen OP, Orrenius S, Bolcsfoldi G, Cotgreave IA (2003) Visualization of the compartmentalization of glutathione and protein–glutathione mixed disulfides in cultured cells. FASEB J 17:124–126
29. Trudel S, Stewart AK, Li Z, Shu Y, Liang SB, Trieu Y, Reece D, Paterson J, Wang D, Wen XY (2007) The Bcl-2 family protein inhibitor, ABT-737, has substantial antimyeloma activity and shows synergistic effect with dexamethasone and melphalan. Clin Cancer Res 13:621–629
30. Tyurina YY, Tyurin VA, Yalowich JC, Quinn PJ, Claycamp HG, Schor NF, Pitt BR, Kagan VE (1995) Phenoxyl radicals of etoposide (VP-16) can directly oxidize intracellular thiols: protective versus damaging effects of phenolic antioxidants. Toxicol Appl Pharmacol 131:277–288
31. Voehringer DW, McConkey DJ, McDonnell TJ, Brisbay S, Meyn RE (1998) Bcl-2 expression causes redistribution of glutathione to the nucleus. Proc Natl Acad Sci USA 95:2956–2960
32. Voehringer DW, Meyn RE (2000) Redox aspects of Bcl-2 function. Antioxid Redox Signal 2:537–550
33. Yin DX, Schimke RT (1995) BCL-2 expression delays drug-induced apoptosis but does not increase clonogenic survival after drug treatment in HeLa cells. Cancer Res 55:4922–4928
34. Yu C, Rahmani M, Almenara J, Sausville EA, Dent P, Grant S (2004) Induction of apoptosis in human leukemia cells by the tyrosine kinase inhibitor adaphostin proceeds through a RAF-1/MEK/ERK- and AKT-dependent process. Oncogene 23:1364–1376
35. Zimmermann AK, Loucks FA, Schroeder EK, Bouchard RJ, Tyler KL, Linseman DA (2007) Glutathione binding to the Bcl-2 homology-3 domain groove: a molecular basis for Bcl-2 antioxidant function at mitochondria. J Biol Chem 282:29296–29304